

Uranium groundwater anomalies and active normal faulting

W. Plastino · G. F. Panza · C. Doglioni · M. L. Frezzotti · A. Peccerillo ·
P. De Felice · F. Bella · P. P. Povinec · S. Nisi · L. Ioannucci · P. Aprili ·
M. Balata · M. L. Cozzella · M. Laubenstein

Received: 29 September 2010
© Akadémiai Kiadó, Budapest, Hungary 2010

Abstract The ability to predict earthquakes is one of the greatest challenges for Earth Sciences. Radon has been suggested as one possible precursor, and its groundwater anomalies associated with earthquakes and water–rock interactions were proposed in several seismogenic areas worldwide as due to possible transport of radon through microfractures, or due to crustal gas fluxes along active faults. However, the use of radon as a possible earthquake’s precursor is not clearly linked to crustal deformation. It is shown in this paper that uranium groundwater anomalies, which were observed in cataclastic rocks crossing the underground Gran Sasso National Laboratory, can be used as a possible strain meter in domains where continental lithosphere is subducted. Measurements evidence clear, sharp anomalies from July, 2008 to the end of March, 2009, related to a preparation phase of the seismic

swarm, which occurred near L’Aquila, Italy, from October, 2008 to April, 2009. On April 6th, 2009 an earthquake ($M_w = 6.3$) occurred at 01:33 UT in the same area, with normal faulting on a NW–SE oriented structure about 15 km long, dipping toward SW. In the framework of the geophysical and geochemical models of the area, these measurements indicate that uranium may be used as a possible strain meter in extensional tectonic settings similar to those where the L’Aquila earthquake occurred.

Keywords Earthquake · Seismogenic areas · Groundwater · Uranium · L’Aquila earthquake · Italy

W. Plastino (✉) · F. Bella
Department of Physics, University of Roma Tre, Rome, Italy
e-mail: plastino@fis.uniroma3.it

W. Plastino
National Institute of Nuclear Physics, Section of Roma Tre,
Rome, Italy

G. F. Panza
Department of Earth Sciences, University of Trieste, Trieste,
Italy

G. F. Panza
Abdus Salam International Centre for Theoretical Physics,
Trieste, Italy

C. Doglioni
Department of Earth Sciences, University of Roma
“La Sapienza”, Rome, Italy

M. L. Frezzotti
Department of Earth Sciences, University of Siena, Siena, Italy

A. Peccerillo
Department of Earth Sciences, University of Perugia, Perugia,
Italy

P. De Felice · M. L. Cozzella
Department of Environment, ENEA, National Institute
for Metrology of Ionizing Radiations, Rome, Italy

P. P. Povinec
Department of Nuclear Physics and Biophysics,
Comenius University, Bratislava, Slovakia

S. Nisi · L. Ioannucci · P. Aprili · M. Balata · M. Laubenstein
National Institute of Nuclear Physics,
Gran Sasso National Laboratory, Assergi, AQ, Italy

Introduction

Earthquake prediction, due to its societal relevance and the intrinsic complexity of the problem, has been the subject of several controversial discussions and reviews [1–4]. The geodynamic processes leading to earthquakes can modify radon migration patterns in groundwater that could be used as a potential strain meter probe [5]. Radon (Rn) as a possible candidate for earthquake's precursor has been studied for a long time, but there is no clear evidence that it is really a precursor [6]. It has been suggested as one of several possible early signals, and its air or groundwater anomalies associated with earthquakes and air–rock or water–rock interactions were detected in several seismogenic areas worldwide [7–18].

The physical processes associated with Rn anomalies are based on the changes of Rn emanation rates occurring due to strain signal near to the earthquake's nucleation point. Particularly, its behaviour before, during and after the main shock, considering the consolidated scheme for Rn release due to stress–strain processes in the rock is unclear. In the geological environment, the Rn concentration depends on the isotopic abundance of its parent radionuclides (^{238}U and ^{226}Ra), and on their geochemical patterns with reference to environmental redox and pH characteristics. The geodynamic processes induced by earthquakes can modify Rn migration patterns as a potential indicator of strain. However, the activity of Rn in fractured lithologies is difficult to predict, and the Rn concentration does not uniquely constrain the rock deformation or the chemical inhomogeneity nor its relationship with the transient crustal strain signals from 'aseismic' fault slip, near to the earthquake's nucleation point [6]. Moreover, non-tectonic factors related to variations of chemical and physical groundwater parameters may be of importance and proper geological, hydrological and hydrogeological settings [16] are required to isolate the variations induced by stress–strain processes.

Materials and methods

Sampling

The Gran Sasso National Laboratory of the National Institute of Nuclear Physics (LNGS–INFN) is located in the Gran Sasso massif (central Apennines, Italy) inside the largest aquifer of central Italy, within Mesozoic carbonates. These rocks have been deformed and fractured during an earlier Miocene–Pliocene compressive phase. Since Pleistocene, the massif has been cross-cut by normal faults [17].

Groundwater to be analyzed flows in pipes introduced into the rock up to a depth ranging from 3 to 6 m. Water

samples were collected weekly in four sites located inside the LNGS–INFN. Each 1L sample was stored, in cleaned and rinsed polyethylene bottles, after 5 min of water flushing at maximum flow.

ICP-MS

The water samples were diluted 10 times and acidified with 2.5% of nitric acid to stabilize traces in the sample. During sampling reagents of trace analysis grade (HNO_3 super pure by Carlo Erba[®] Reagenti), ultra pure water (produced by Millipore MilliQ[®]-Element), plastic containers and ancillary equipment were used as long-lived radionuclides Th and U at trace levels had to be measured. The ICP-MS measurements were carried out using a quadrupole mass spectrometer from Agilent[®] Technologies, model 7500a. The tuning of the instrument was optimized in order to reach high sensitivity, stable signal, and low background. A Babbington nebulizer was used during the measurements. The concentration values were determined in quantitative mode using an external calibration curve, because the matrix effect of the ten times diluted groundwater samples is negligible. During the measurements a multi-element solution was used as the internal standard to correct for possible instability and drift of the ICP-MS device. This solution was added on line using the third line of the peristaltic pump. The calibration curve of U response was corrected using ^{209}Bi . The accuracy reached in this way, as a rule, was better than 5%, which is reasonable for the ICP-MS technique.

Results and discussion

Within the framework of the INFN's scientific program ERMES (Environmental Radioactivity Monitoring for Earth Sciences) radon (^{222}Rn) [17], radiocarbon (^{14}C) [19] and tritium (^3H) [20] have been monitored in the groundwater inside the LNGS–INFN, and different chemical, physical and fluid dynamical characteristics of groundwater have been measured. The uranium (U) groundwater monitoring started on June 2008 with the aim of better defining the Rn groundwater transport processes through the cataclastic rocks [17], as well as to check its contribution to the neutron background at the LNGS–INFN [21]. The U measurements (Fig. 1) carried out between June 2008 and May 2010 at four different sites (E1, E4 and E3, E3dx) show the presence of two different water groups, whose existence is confirmed by stable isotope of hydrogen and oxygen ($\delta^2\text{H}$, $\delta^{18}\text{O}$), ^{14}C and ^3H analyses [22].

A seismic swarm, whose main shock occurred at 01:33 UT on April 6th, 2009, has affected the area under investigation from October 2008 to April 2009. The main

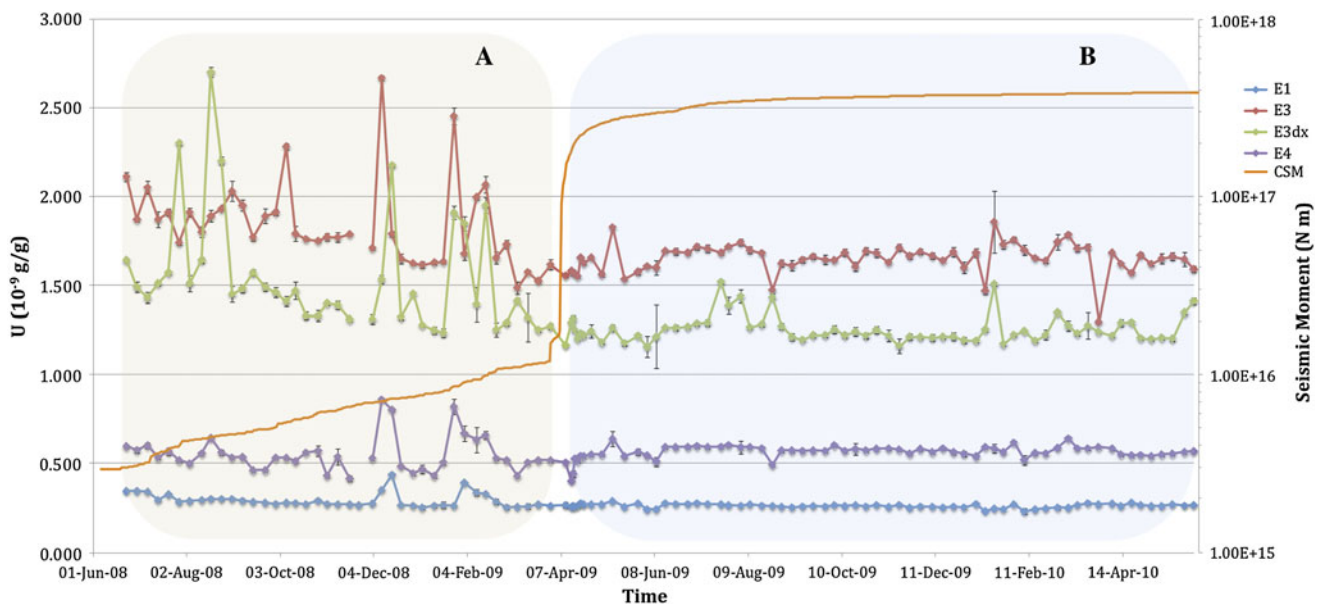


Fig. 1 Time variation of U concentration in groundwater sampled at E1, E3, E3dx, and E4 from June 2008 to May 2010. In the period A, from 23rd June 2008 to 31st March 2009, these readings show a clear short-term 40–80% peak structure. In the period B, from 10th April 2009 to 31st May 2010, the systematic peak structure for U is no longer present. A seismic swarm started in the area under

investigation, whose main shock occurred at 01:33 UT on April 6th, 2009. The cumulative seismic moment (CSM) from January 2008 to May 2010 in the area 42.00–42.75°N and 12.75–13.75°E has been estimated from seismic data of the Italian Seismic Bulletin, Istituto Nazionale di Geofisica e Vulcanologia: the clear jump in the CSM coincides with the main shock on April, 6th, 2009

($M_w = 6.3$) event is located about 18 km far from LNGS–INFN. After 6th April, 2009 the seismicity continued and migrated to the N and SE sectors, with two aftershocks of $M_w = 5.2$ and $M_w = 5.4$. Until 31st May 2010 more than 15,000 events with magnitudes greater than 1.0 with depth between 6 and 20 km have been recorded in the area 42.00–42.75°N and 12.75–13.75°E.

Simultaneous measurements of the following parameters were performed for each water sample at the monitoring sites inside the LNGS–INFN: U, sodium (Na), magnesium (Mg), potassium (K), calcium (Ca), electrical conductivity (EC), oxidation–reduction Potential (ORP), and pH. Some 110 parallel readings were recorded and each series was normalized to the corresponding average. The U, Na, Mg, K and Ca readings show a long-term variability, around the unit value, limited to $\pm 20\%$. In addition to this background, in the period A, from 23rd June 2008 to 31st March 2009, these readings show a clear short-term 40–80% peak structure. In this period, relative to site E3dx for example, the experimental relative standard deviations (RSD) are about 20–25% for U, Na, Mg and Ca, and 35% for K that shows the largest peaked short-term variations, as well. Readings of EC, ORP and pH show relatively smooth fluctuations within $\pm 10\%$. RSD values vary between 2 and 5% and these quantities are excluded from further analysis.

Readings of Na, Mg, Ca and K were all normalized to the relevant U readings, in order to remove the common

peak structure. The RSD of these ratios are 10% (Na), 9% (Mg), 7% (Ca) and 3% (K). Considering the Na/U ratio, with RSD of 0.10 and the two individual Na and U variability, both about 0.24, the Na–U covariance was estimated to be about 0.05. This is confirmed by the experimental covariance between each reading and the U ones, obtained from the set of data: 0.049 (Na), 0.046 (Mg), 0.047 (Ca). It is then evident that U, Na, Mg, Ca and K readings are correlated (Table 1).

A different situation can be observed in period B, from 10th April 2009 to 31st May 2010. The systematic peak structure for U, Na, Mg, Ca and K readings is no longer present, and only few isolated peaks of K and Na can now be observed. This is confirmed by the data presented in Table 1. As an example, relative again to site E3dx, the RSD have been reduced to about 5% for U, Mg and Ca, and 15% for K and Na. These values agree well with the corresponding RSD of normalized (to U) readings in period A, typical of the constant background variability of periods A and B.

Period B readings of EC, ORP and pH show a similar behavior as in period A, with RSD values between 2 and 5%. In both periods the pH reported the minimum RSD of 1.7 and 1.1%. The covariance analysis confirms this finding. Indeed, because of the loss of the peak structure, the correlation coefficients between each reading and the U ones are reduced from 0.88 (Na), 0.91 (Mg), 0.75 (K), 0.93 (Ca) to 0.31 (Na), 0.50 (Mg), 0.19 (K), 0.56 (Ca).

Table 1 Summary of statistical analysis (Relative Standard Deviation, Mean, Covariance and Correlation with U) for each site and simultaneous readings of U, Na, Mg, K, Ca, EC, ORP, and pH, during the periods A (from 23rd June 2008 to 31st March 2009) and B (from 10th April 2009 to 31st May 2010). Each series was normalized to the corresponding average

	U	Na	Mg	K	Ca	EC	ORP	pH
A								
E1								
RSD	0.145	0.148	0.134	0.272	0.130	0.026	0.063	0.024
Mean	1.073	1.079	1.015	1.081	1.030	0.967	0.987	1.014
Cov (U, X)	0.020	0.019	0.017	0.027	0.016	0.000	-0.002	-0.001
Corr (U, X)	1.000	0.935	0.877	0.714	0.886	-0.095	-0.236	-0.174
E3								
RSD	0.139	0.158	0.137	0.419	0.132	0.024	0.047	0.025
Mean	1.072	1.075	1.022	1.105	1.040	0.973	1.038	1.002
Cov (U, X)	0.019	0.019	0.016	0.029	0.017	0.000	0.000	0.000
Corr (U, X)	1.000	0.874	0.851	0.517	0.937	-0.062	-0.033	0.023
E3dx								
RSD	0.241	0.240	0.221	0.366	0.219	0.022	0.046	0.017
Mean	1.134	1.099	1.066	1.143	1.092	0.987	1.032	1.003
Cov (U, X)	0.057	0.050	0.047	0.065	0.048	0.000	0.000	-0.001
Corr (U, X)	1.000	0.884	0.906	0.752	0.931	-0.019	0.019	-0.130
E4								
RSD	0.183	0.171	0.150	0.403	0.165	0.030	0.053	0.021
Mean	0.967	1.069	1.033	1.175	1.051	0.979	1.076	0.999
Cov (U, X)	0.033	0.024	0.023	0.046	0.026	0.000	0.002	0.000
Corr (U, X)	1.000	0.775	0.872	0.645	0.896	0.080	0.267	-0.127
B								
E1								
RSD	0.041	0.036	0.035	0.088	0.036	0.026	0.054	0.008
Mean	0.956	0.952	0.991	0.952	0.982	1.020	1.008	0.991
Cov (U, X)	0.002	0.001	0.000	0.000	0.000	0.000	0.000	0.000
Corr (U, X)	1.000	0.400	0.181	0.141	0.309	0.002	0.173	-0.102
E3								
RSD	0.049	0.040	0.034	0.108	0.038	0.021	0.057	0.012
Mean	0.957	0.956	0.986	0.928	0.977	1.016	0.977	0.999
Cov (U, X)	0.002	0.000	0.000	0.000	0.000	0.000	0.000	0.000
Corr (U, X)	1.000	0.115	0.074	-0.010	-0.081	0.138	-0.148	-0.033
E3dx								
RSD	0.056	0.132	0.043	0.157	0.040	0.026	0.053	0.011
Mean	0.920	0.940	0.961	0.919	0.946	1.008	0.982	0.998
Cov (U, X)	0.003	0.002	0.001	0.002	0.001	0.000	0.001	0.000
Corr (U, X)	1.000	0.309	0.496	0.193	0.554	0.226	0.302	-0.460
E4								
RSD	0.069	0.045	0.041	0.103	0.040	0.023	0.062	0.021
Mean	1.009	0.959	0.980	0.904	0.970	1.013	0.955	1.001
Cov (U, X)	0.005	0.002	0.002	0.003	0.001	0.001	0.001	0.000
Corr (U, X)	1.000	0.624	0.554	0.419	0.470	0.356	0.271	-0.158

The water–rock interaction, modulated by percolation processes (due to meteoric events) above the water table of the Gran Sasso aquifer, do not justify the U anomalies [22]. Therefore, the progressive marked increase of U, along

with the enrichment in Ca, Mg, and Na observed in groundwater located close to the main fault, crossing the deep underground LNGS–INFN during the preparation phases of the recent L’Aquila earthquake of 6th April 2009,

is interpreted as chemical interactions with endogenic, upper mantle-derived carbon dioxide (CO₂) fluids, generated by recycling and melting of carbonaceous sediments during the ongoing subduction of the continental Adriatic plate beneath the Italian peninsula [23].

Recent evidences [24] indicate a shallow upper mantle convection/circulation [25] related to metasomatism and melting, and confirm the “west to east” flow of the mantle relative to the lithosphere, as suggested by the Apennines slab eastward retreat [26]. This flow is consistent with the shear-wave splitting analysis that indicates an E-W upper mantle anisotropy [27, 28] due to the olivine crystals preferred orientation induced by mantle flow. The changes in the crustal stress pattern and stress magnitude are likely to be caused by buoyancy driven mantle circulation in the region rather than by gravitational potential energy differences (due to lateral density variations) in the crust itself [29]. The combined analysis of petrological, geochemical and geophysical data reveals a surprisingly consistent picture showing that variations of seismic waves velocity in the mantle could be related to compositional differences of mantle sources, and not only to pressure and temperature variations [30]. Petrological and geophysical modeling [31] explains how carbon is efficiently cycled in the upper mantle beneath Italy and the Western Mediterranean region at the Ma scale, via low-fractions of carbonate melts (about 0.1 wt%) generated by melting of carbonate-rich lithologies of the subducted Adria lithosphere, induced by the progressive rise of mantle temperatures behind the eastward-retreating subducting plate (Fig. 2). The extraction of small-degree carbonate melts produces an abundant source of metasomatic fluids. Fluxes of carbonate melts are Na-bearing dolomitic (MgCaCO₃) in composition and contain from a hundred up to a thousand times the concentration in noble gases, heat-producing elements (e.g., U, Th and K, and other very incompatible elements, Cs, Rb, and Ba) than the primitive mantle [23].

Experimental petrology data [32] indicate that the generation of carbonate-rich melts beneath the Western Mediterranean and Italy commences at depths of 150–120 km. Due to their low density and viscosity, such melts are extremely mobile and migrate upward through the mantle, forming a carbonated partially molten CO₂-rich mantle, recorded by tomographic images between 120 and 60 km depth [30, 31]. The upwelling of carbonate-rich melts to depths less than 60–70 km (i.e., below their P–T stability field) induces a massive outgassing of CO₂ in the lithosphere. Buoyancy forces, probably favored by fluid overpressures, are able to allow its migration to the exosphere through deep lithospheric faults, especially in the zones of thinned continental crust [31] (e.g., “non volcanic” CO₂ soil degassing in Tuscany and Latium).

However, not all of the CO₂ formed at mantle depth may reach the surface: some could remain trapped beneath the Moho and within the lower crust, in zones characterized by a thickened continental crust and lithosphere. Crustal CO₂ confinement might naturally give rise to over-pressurized reservoirs enriched in rare gases, Th, U and K, and other very incompatible elements, which are known to facilitate, in normal fault areas, seismogenesis, like the Colfiorito 1997 earthquake [33, 34].

The mechanic of faults is strongly influenced by fluids, their pore pressure, chemistry (e.g., CO₂, H₂O, etc.) and the resulting variation of friction along the fault plane [34, 35]. Fluids may be actively triggering the rupture, and they are passively squeezed out during seismic events. Mantle CO₂ confined in the lower-middle crust is a chemically powerful agent for shallow aquifers. Discontinuous inputs of very low amounts (in the order of 1 mol % or less), induced by the progressive increase of CO₂ fluxes in zones of active faulting, are sufficient to give the aquifers the capability to dissolve carbonate bed/wallrocks, which should result in a spiked load of Mg and Ca, associated to an enrichment in U and other incompatible elements, similar to the geochemical patterns evidenced by the monitoring discussed here.

GPS data [36] show that, at global scale, a large part of deformation is absorbed by viscous shear in the lower crust. Such steady-state deformation contrasts with the stick–slip behavior of faults such as the one that generated the April 6th, 2009 event. Therefore, during the interseismic period, the lower crust, below the brittle–ductile transition, is constantly sheared, while faults in the upper crust are locked. During this time interval, the volume of rocks located at the brittle–ductile transition should suffer dilatancy, generated by the differential motion of the lower crust relative to the inactive upper crustal segment of the fault. Fluids are expected to fill in the fractures formed during the interseismic period. The separation produces a weak volume of rocks that sustain the hanging wall of the normal fault only until the load of the brittle upper crust will not overtake the strength of the dilated rocks. At that point, the hanging wall suddenly falls down to refill the stretched volume. This process implies the increase in pore pressure and the squeezing out of fluids. The hanging wall is expected to gradually adjust to its new position, generating a long sequence of aftershocks as those observed after the M_w 6.3 April 6th, 2009 L’Aquila earthquake. Some 15 km SW from the fault zone where LNGS–INFN is located, the area is cross-cut by several NW–SE trending active normal faults [37] cross-cutting the carbonatic massif of the Gran Sasso, where a sudden increase of fluid discharge has been observed during the main earthquake.

Although U concentrations and ²³⁴U/²³⁸U isotope ratios have been monitored in thermal waters [38–40], in order to assess the validity of U isotopes as fluid phase earthquake

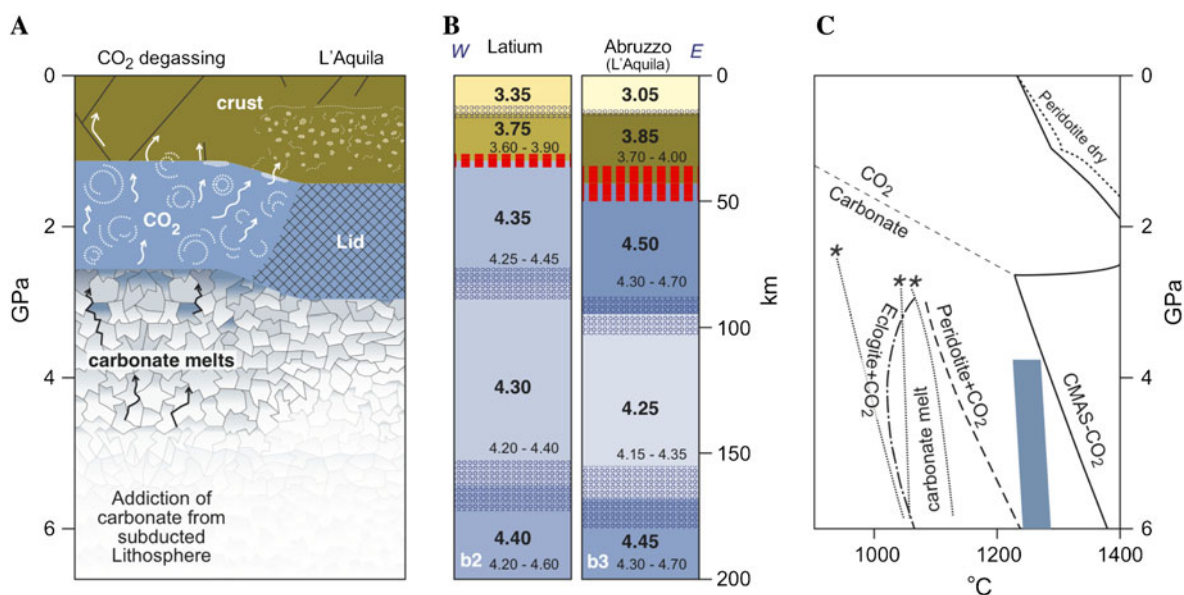


Fig. 2 Present-day architecture of mantle- CO_2 degassing beneath L'Aquila (Central Italy). The generation and evolution of deep mantle-derived CO_2 (A) has been delineated integrating surface wave tomography (B) with experimentally determined melting relationships for carbonated peridotite and crustal lithologies, relevant to recent mantle processes in the Western Mediterranean region (C) [23, 30, 31]. A Geochemical reconstruction (0–200 km depth) beneath the Latium–Abruzzo (L'Aquila) region (Central Italy). B Models [24] of shear-wave velocities (km s^{-1}) versus depth for Latium (b2) and Abruzzo (L'Aquila) zones (b3); the *shadowed areas* indicate the range of variability of the thickness of the layers, the *red dashed lines* mark the range of variability of the Moho depth; this representation is used to evidence that the boundaries between layers can well be transition zones in their own right. C Pressure–temperature diagram showing the effects of CO_2 on upper mantle lithologies [31]. Peridotite- CO_2 solidus; Peridotite- CO_2 and Dry Peridotite solidi in

the CMSA system; Eclogite- CO_2 solidus. KNCFMASH- CO_2 solidus (carbonated pelite + 1.1 wt% H_2O + 4.8 wt% CO_2). Blue area represents the estimated present day mantle temperatures at the inferred pressures. Melting of sediments and/or continental crust of the subducted Adriatic lithosphere at pressures greater than 4 GPa (120 km) and temperatures of 1200 °C (c—blue area) generate carbonate-rich melts. Such melts, migrating upward through the mantle, form a carbonated partially molten layer recorded by tomographic images between 70 and 160 km of depth (B—cell b2) [30]. Further upwelling of carbonate-rich melts induces massive outgassing of CO_2 in the lithospheric mantle (C—carbonate- CO_2 field boundary). High velocities in the uppermost mantle beneath Abruzzo (L'Aquila) support evidence for a LID initiating to subduct toward the west. Beneath Latium, at the same depth, an asthenospheric mantle wedge is present, as indicated by the quite low V_s between 40 and 80 km of depth (LID; B—cell b3) [30]. (Color figure online)

precursors, the monitoring at LNGS–INFN was performed in a shallow aquifer with a high dynamic behavior due to the high permeability of the Mesozoic limestones that form part of the Gran Sasso massif [17].

Conclusions

We propose that the U groundwater anomalies observed before the seismic swarm and the main shock, which occurred on 6th April, 2009 in L'Aquila, provide a key geochemical signal of a progressive increase of deep CO_2 fluxes at middle-lower crustal levels. Repeated sharp U enrichments in groundwater, that can be directly associated with the geodynamics of the earthquake, represent a much more precise strain-meter than Rn, whose presence could be modulated by U content during the preparation phase of the earthquake, and only successively released by microfracturing, during the main shock and aftershocks.

We believe that the U groundwater anomalies observed before the L'Aquila earthquake will trigger further research on geodynamics and hydrogeochemistry of earthquakes, important for better understanding of preparatory and final stages of earthquakes, and for possible routine use of groundwater earthquake precursors.

Acknowledgments The authors greatly acknowledge the support by National Scientific Committee Technology of the National Institute of Nuclear Physics, the Chemistry and Chemical Plants Service of the Gran Sasso National Laboratory, and the Istituto Nazionale di Geofisica e Vulcanologia–Italian Seismic Bulletin for the seismic data.

References

- Geller RJ et al (1997) Earthquakes cannot be predicted. *Science* 275:1616–1617
- Wyss M (1997) Cannot earthquakes be predicted? *Science* 278:487–488
- Nature debates (1999) http://www.nature.com/nature/debates/earthquake/quake_frameset.html

4. Peresan A et al (2005) Intermediate-term middle-range earthquake predictions in Italy: a review. *Earth Sci Rev* 69:97–132
5. Hauksson E (1981) Radon content of groundwater as an earthquake precursor: evaluation of worldwide data and physical basis. *J Geophys Res* 86:9397–9410
6. Roeloffs E (1999) Radon and rock deformation. *Nature* 399:104–105
7. Ulomov VI, Mavashev BZ (1968) On a precursor of a strong tectonic earthquake. *Dokl Akad Sci USSR, Earth Sci Sec* 174:9–11
8. Wakita H, Nakamura Y, Notsu K, Noguchi M, Asada T (1980) Radon anomaly: a possible precursor of the 1978 Izu-Oshima-kinkai earthquake. *Science* 207:882–883
9. King CY (1981) Do radon anomalies predict earthquakes? *Nature* 293:262
10. Wakita H, Igarashi G, Nakamura Y, Sano Y, Notsu K (1989) Coseismic radon changes in groundwater. *Geophys Res Lett* 16:417–420
11. Torgersen T, Beniot J, Mackie D (1990) Controls on groundwater Rn-222 concentrations in fractured rock. *Geophys Res Lett* 17:845–848
12. Monnin MM, Seidel JL (1992) Radon in soil-air and groundwater related to major geophysical events: a survey. *Nucl Instrum Methods A* 314:316–330
13. Virk HS, Singh B (1994) Radon recording of Uttarkashi earthquake. *Geophys Res Lett* 21:737–740
14. Igarashi G et al (1995) Groundwater radon anomaly before the Kobe earthquake in Japan. *Science* 269:60–61
15. King CY, Koizumi N, Kitagawa Y (1995) Hydrogeochemical anomalies and the 1995 Kobe earthquake. *Science* 269:38–39
16. Trique M, Richon P, Perrier F, Avouac JP, Sabroux JC (1999) Radon emanation and electric potential variations associated with transient deformation near reservoir lakes. *Nature* 399:137–141
17. Plastino W, Bella F (2001) Radon groundwater monitoring at underground laboratories of Gran Sasso (Italy). *Geophys Res Lett* 28:2675–2678
18. Richon P et al (2003) Radon anomaly in the soil of Taal volcano, the Philippines: a likely precursor of the M 7.1 Mindoro earthquake (1994). *Geophys Res Lett* 30:1481–1484
19. Plastino W, Kaihola L, Bartolomei P, Bella F (2001) Cosmic background reduction in the radiocarbon measurements by liquid scintillation spectrometry at the underground laboratory of Gran Sasso. *Radiocarbon* 43:157–161
20. Plastino W et al (2007) Tritium in water electrolytic enrichment and liquid scintillation counting. *Radiat Meas* 42:68–73
21. Plastino W et al (2009) Environmental radioactivity in the ground water at the Gran Sasso National Laboratory (Italy): a possible contribution to the variation of the neutron flux background. *J Radioanal Nucl Chem* 282:809–813
22. Plastino W et al (2010) Uranium groundwater anomalies and L'Aquila earthquake, 6th April 2009 (Italy). *J Environ Radioact* 101:45–50
23. Peccerillo A (2005) Plio-Quaternary volcanism in Italy. *Petrology, geochemistry, geodynamics*. Springer, Heidelberg, pp 1–365
24. Panza GF, Raykova RB, Carminati E, Doglioni C (2007) Upper mantle flow in the Western Mediterranean. *Earth Planet Sci Lett* 257:200–214
25. Faccenna C, Jolivet L, Piromallo C, Morelli A (2003) Subduction and the depth of convection in the Mediterranean mantle. *J Geophys Res* 108:2099–2111
26. Gueguen E, Doglioni C, Fernandez M (1998) On the post-25 Ma geodynamic evolution of the Western Mediterranean. *Tectonophysics* 298:259–269
27. Margheriti L, Lucente FP, Pondrelli S (2003) SKS splitting measurements in the Apenninic–Tyrrhenian domain (Italy) and their relation with lithospheric subduction and mantle convection. *J Geophys Res* 108:2218–2237
28. Barruol G, Deschamps A, Coutant O (2004) Mapping upper mantle anisotropy beneath SE France by SKS splitting indicates Neogene asthenospheric flow induced by Apenninic slab rollback and deflected by the deep Alpine roots. *Tectonophysics* 394:125–138
29. Ismail-Zadeh A, Aoudia A, Panza GF (2010) Three-dimensional numerical modeling of contemporary mantle flow and tectonic stress beneath the Central Mediterranean. *Tectonophysics* 482:226–236
30. Panza GF, Peccerillo A, Aoudia A, Farina B (2007) Geophysical and petrological modeling of the structure and composition of the crust and upper mantle in complex geodynamic settings: the Tyrrhenian Sea and surroundings. *Earth Sci Rev* 80:1–46
31. Frezzotti ML, Peccerillo A, Panza GF (2009) Carbonate metasomatism and CO₂ lithosphere-asthenosphere degassing beneath the Western Mediterranean: an integrated model arising from petrological and geophysical data. *Chem Geol* 262:108–120
32. Thomsen TB, Schimidt MW (2008) Melting of carbonated pelites at 2.5–5.0 GPa, silicate–carbonate liquid immiscibility, and potassium–carbon metasomatism of the mantle. *Earth Planet Sci Lett* 267:17–31
33. Chimera G, Aoudia A, Saraò A, Panza GF (2003) Active tectonics in Central Italy: constraints from surface wave tomography and source moment tensor inversion. *Phys Earth Planet Int* 138:241–262
34. Miller S et al (2004) Aftershock driven by a high pressure CO₂ source at depth. *Nature* 427:724–727
35. Sibson RH (1992) Implications of fault-valve behaviour for rupture nucleation and recurrence. *Tectonophysics* 211:283–293
36. Kreemer C, Holt WE, Haines AJ (2002) The global moment rate distribution within plate boundary zones. *Geodyn Ser* 30:173–189
37. Vezzani L, Ghisetti F (1998) Carta Geologica dell'Abruzzo - scala 1/100.000. Regione Abruzzo, Selca
38. Kuleff I, Petrov P, Kostadinov K (1980) Uranium content variations in thermal waters from the west Rhodope crystalline massif during earthquakes in the Chepina valley (south Bulgaria). *J Radioanal Nucl Chem*. 58:267–274
39. Finkel RC (1981) Uranium concentrations and ²³⁴U/²³⁸U activity ratios in fault associated groundwater as possible earthquake precursors. *Geophys Res Lett* 8:453–456
40. McCaig A (1989) Fluid flow through fault zones. *Nature* 340:600